ISSN 0543-5846
METABK 64(1-2) 53-56 (2025)
UDC:621.876:621.462./515.1:518.1=111

NUMERICAL ANALYSIS OF THE ELEVATOR BOOSTING PERFORMANCE OF FLAT-TUBE-AND-FIN HEAT EXCHANGER

Received – Primljeno: 2024-06-12
Accepted – Prihvaćeno: 2024-08-15
Original Scientific Paper – Izvorni znanstveni rad

In this work, elevators shaped by NACA 0012 were deployed on the outer surfaces of tubes in a Flat-tube-and-fin heat exchanger, and their structural details were numerically investigated. Then, following an infrared experiment validation, heat transfer coefficient, pressure loss and JF factor were numerically compared to confirm performance enhancement. It is found that the maximum deviations between numerical and experimental data, 6,31 % of heat transfer coefficient and 3,84 % of pressure loss, secure the accuracy of the following comparison, and the maximum increases of heat transfer coefficient, pressure loss, and JF factor are 7,20 %, 0,07 %, and 7,09 % at 12 m/s, respectively.

Keywords: Flat-tube-and-fin heat exchanger, NACA 0012, performance enhancement, elevator, CFD

INTRODUCTION

Flat-tube-and-fin heat exchanger (FTFHE) is widely used in vehicle, especially for the off-road vehicle working under severe working conditions, due to its better structural strength, dust avoiding performance and high efficiency. Driven by overwhelming assignments, more powerful engines appear in related machine design. As a consequence, how to dissipate the overheating brought by these engines becomes a challenge to designers and researchers. Among the implementations on the air side of radiators, a welcome option is to replace or change geometrical shapes of tubes [1-4], so the flow resistance of air could be rapidly reduced as heat exchange fluctuates slightly. However, there is limited research on the tubes from heat exchanger, which was also pointed out by Tahaseen et al. [5] in the summary of related works.

The performance of heat exchanger mainly features pressure loss and heat dissipation, and a better performance usually relies on reduced pressure loss, increased heat dissipation or the combination of both. By the airflow guiding of elevator, this work inclines to enhance the heat transfer of FTFHE with NACA 0012-shaped elevator at the acceptable cost of pressure loss.

NUMERICAL ANALYSIS OF THE PROPOSAL MODEL

Based on the structural data from Tables 1 and 2, a 3D elementary unit of FTFHE was completed with the commercial modeling software, and its schematic diagram is shown in Figure 1. NACA 0012, a typical symmetrical airfoil, was employed as the geometrical characteristic of elevator, and its mainly involved structural elements were chord, mass point, leading, and trailing edges. Mass point, also defined as orientation point, located on a third of chord length to the leading edge. The detailed schematic diagram of geometrical parameters and the 3D model is depicted in Figure 2, where the local Cartesian coordinate was oriented in the center of the plain surface of the tube. The angle between Axis X and chord was named mounted angle, a_m. The horizontal distance from the coordinate origin to the surface edge near air inlet was defined as $d_{front}=(pf_h-hf_h)/2$, and the vertical distance from the coordinate origin to the top of the lower fin was defined as $d_{lower}=(hf_c-d_c)/2$. The detailed structural parameters of elevator are listed in Table 3.

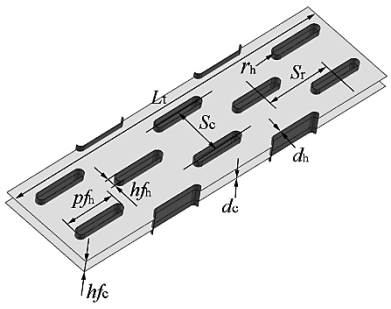

Figure 1 Physical modeling of the elastic shaft section

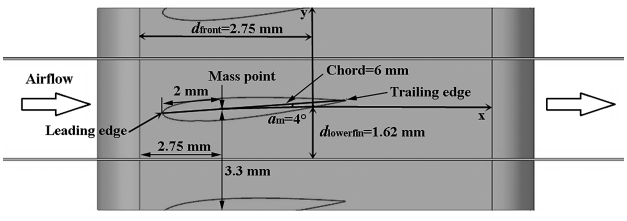

Figure 2 Bearing-rotor contact model

W. T. SHEN[a], Y. F. ZHAO[a], Z. C. XU[a], C. Y. HAN[a], B. Z. WANG[a,b,*], X. C. QIAN[c]
[a] College of Automotive Engineering, Hebei College of Science and Technology, Tangshan 063210, China
[b] College of Mechanical Engineering, North China University of Science and Technology, Tangshan 063210, China
[c] Steelmaking Department, Shougang Jingtang United Iron and Steel Co, Ltd, Tangshan 063210, China (E-mail: wbzhong@ncst.edu.cn)

Table 1 **Structural parameters of the tube**

Parameters	Variable	Value
Tube outer diameter	pf_h	14(slot)
Tube outer diameter	hf_h	2,5
Tube thickness	d_{tube}	0,12
Semicircles radius	$r_h = hf_h/2$	1,25
Transverse pitch	S_{column}	13
Tube amount	N_h	328
Tube row number	N_{hrow}	5
Longitudinal pitch	S_{row}	18

Table 2 **Structural parameters of the air-side fin**

Parameters	Variable	Value
Fin pitch	hf_c	3,3
Fin thickness	d_{fin}	0,06
Fin amount	N_c	262
Total surface area	A_c	44

Table 3 **The detailed structural parameters of elevator**

Name	Variable	Value
Chord length	L_d	6 mm
Vertical distance to upper fin	hf_c-d_{lower}	1,62 mm
Horizontal distance to the rear edge of tube plain surface	pf_h-hf_h-d_{front}	8,75 mm
Mounted angle	a_m	4°
Extruded length of elevator	-	1 mm
Vertical distance to the fin	$d_{lowerfin}$	1,62 mm
Horizontal distance to the fin	d_{front}	2,75 mm

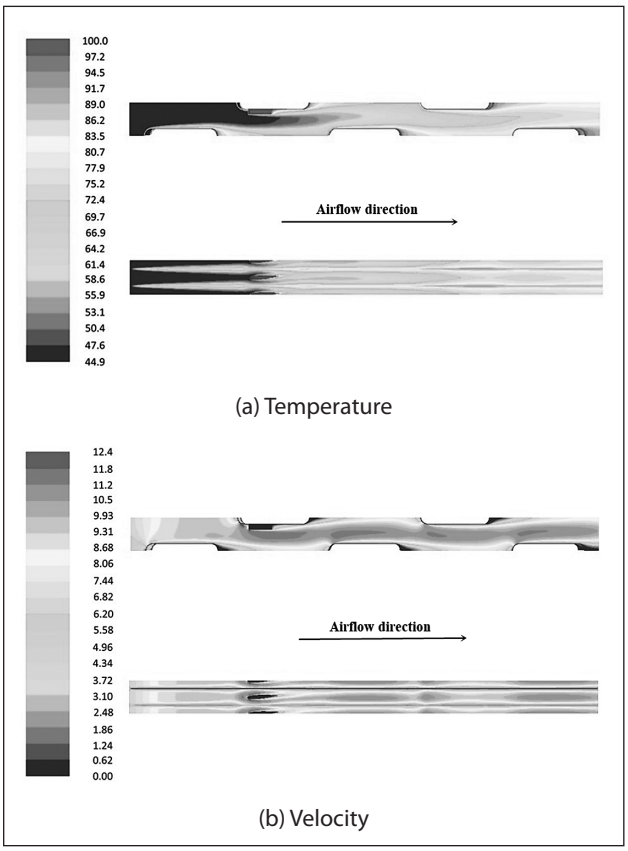

Figure 3 Temperature and velocity distributions

NUMERICAL PREPROCESSING

The inlet and the outlet of the computational domain were extended upstream 1,5 times and downstream 5 times the diameter of the fin, respectively, for a steady flow status. All velocity component were set to be 0, the normal velocity component at symmetry plane was 0, and no-slip conditions for velocity were specified.

GAMBIT 2,4,6 was employed to generate meshing grids meeting the demands from more accurate heat transfer, grid independence, and the minimum consumption of time and other resources. Boundary layer meshing was applied to the air-side surfaces of fin and airfoil, so the deviation brought by rough grids could be lowered down to an applicable level. Structural grid was a preferred choice for fin surfaces, and its transition to boundary layer was repeatedly tested for a more ideal configuration. The 4-layer boundary layer was initialized with 0,005 and a growth rate of 1,1.

Governing equations were taken into the numerical prediction. The iteration was executed by FLUENT 15,0. When the scaled residual of energy equation was consecutively less than 1×10^{-7} in 20,000 iterations, the solution would be considered converged.

For a fair comparison, all the slices of temperature and velocity distributions in this work were extracted from the same parallel position. A high-temperature elevator played a distinct role in Figure 3a. There were two expected functions of the attached elevator for the enhancement of heat transfer. The first one, an extended surface for the heat transfer between air and fin, was taken as an advantage, and complied with the common physical introduction in textbooks. The other one, less energy consumption, happened to be the superiority of airfoil. As an outcome of this working elevator, the average temperature of the air around it was at 67°C and reached 70°C after flowing past the elevator.

The velocity distribution under constant inlet 6 m/s is presented in Figure 3b. As cold air flowed into a narrow section, its velocity increased to 9,93-11,2 m/s. Then, this part of the air initialized its contact with the elevator and flowed along the elevator surfaces. Besides that, as a consequence of a specific mounted angle and orientation point location, the air beneath the elevator kept a consecutive velocity distribution.

EXPERIMENTAL VALIDATION ON THE PROPOSED MODEL

The infrared experimental results are plotted in Figure 4a, where 14 markers together with their corresponding temperatures were assigned to the airflow path inside the test section, while simulation results are shown in Figure 4b. A similar temperature gradient along the airflow direction could be clearly observed in

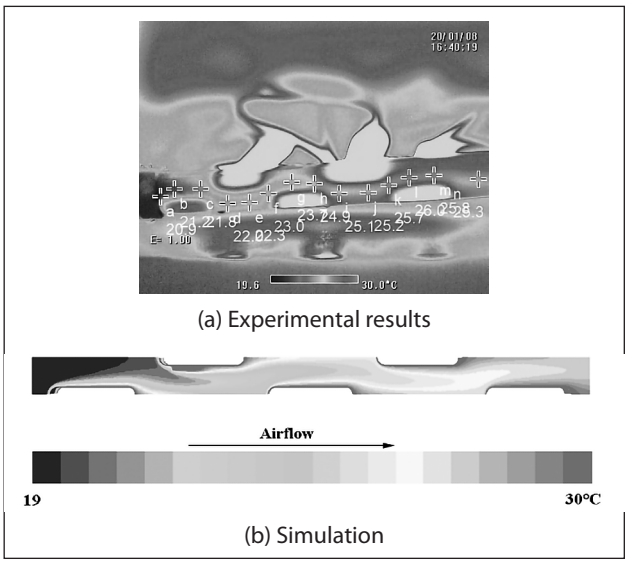

Figure 4 Test and simulation cloud map

both figures. The temperatures at the same markers between two figures showed a good agreement.

COMPARISON BETWEEN ORIGINAL AND IMPROVED SCHEMES

Figure 5a depicts a comparison of the heat transfer coefficients from both models. The comparison stated that, compared with the original model, the improved one possessed a higher heat transfer coefficient over the velocity range of 2-12 m/s. The deviation came to its minimum at 2 m/s and the maximum at 12 m/s, 7,2 %. The main reason for that might be that the cold air with a higher speed increased the transported heat flux between fin and air. Under the perspective of heat transfer, undoubtedly, the elevator worked as expected, which indicated that the working mechanism of guiding air by the elevator was feasible.

Figure 5b presents a comparison of the pressure losses from both models. The difference between the two models remained vague throughout the whole velocity range, and the maximum was 0,07 % at 12 m/s. This difference was so small that the increased pressure loss caused by the elevator could be considered acceptable within a certain tolerance, and it could be explained by the low-resistance characteristics of NACA 0012 airfoil.

Figure 5c introduces a comparison of *JF* factors from both models. Overall, both *JF* factors showed the same downward trend with the increasing inlet velocity of air. Obviously, the *JF* factor from the improved scheme was higher than that from the original one over the velocity range of 2-12 m/s, and their maximum difference was 13,74 % at the inlet velocity of 2 m/s. Then, with a rise in velocity, it remained shrinking down until 7,09 % at 12 m/s. Several reasons might be responsible for that phenomenon. the expanded structure brought by the elevator, the air guiding by elevator, and the low-

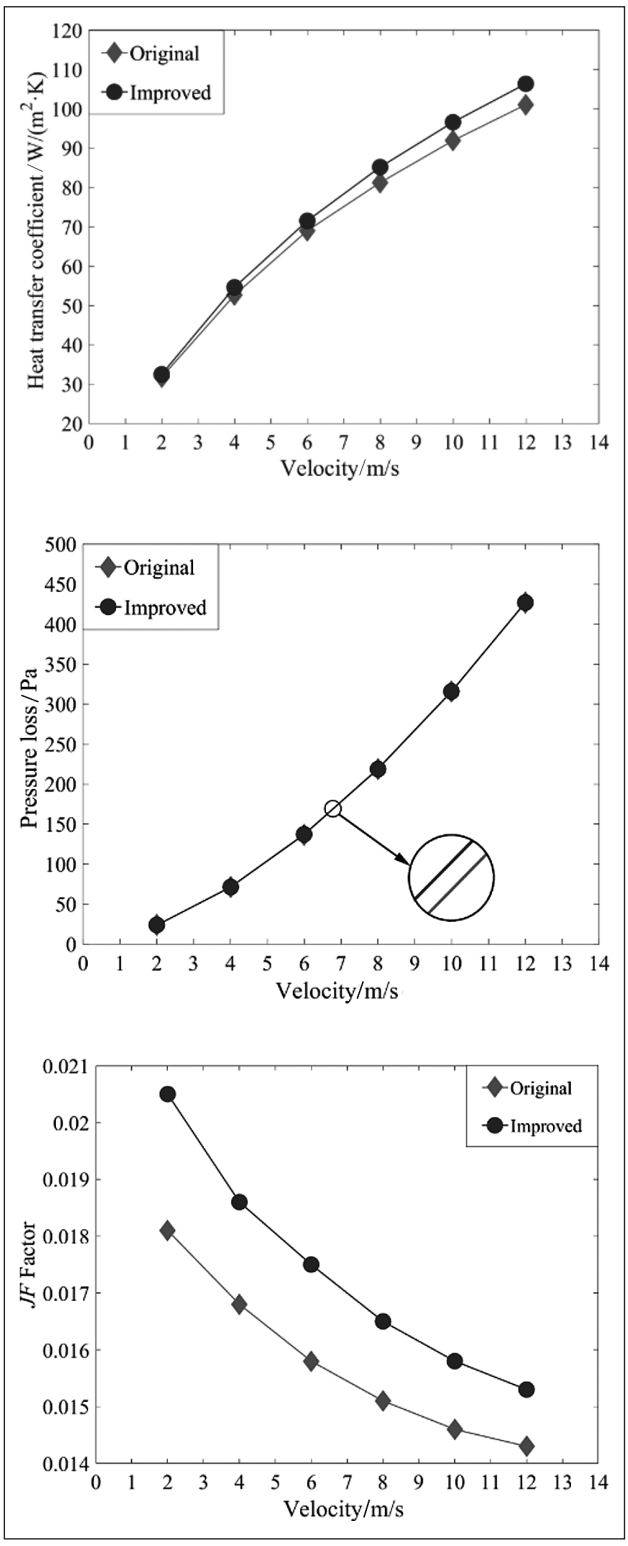

Figure 5 X-direction time-domain map 0,1 mm

resistance characteristics of the geometrical shape of the elevator might account for that enhancement.

CONCLUSION

Inspired by the elevator used for submarine and aircraft, this work investigated the performance enhancement brought by the elevator attached to the tube of

a FTFHE. As a start, a 3d model was established and numerically analyzed. Then, an infrared experiment was performed on the improved model. At last, the heat transfer coefficient, pressure loss, and *JF* factors brought by the elevator were examined. Based on the above work, the following conclusions were made:

(1) One elevator on the second tube to air inlet should be ensured in the improved scheme. As four main geometrical parameters for a NACA 0012 elevator, mounted angle, chord length, extruded length, and orientation point may determine the final modeling and comprehensive performance. When they are 4°, 6 mm, 1 mm, and Point 5, respectively, the improved scheme presents the highest *JF* factor.

(2) The correctness of the employed numerical analysis in this work was validated with infrared experimental data, which could be the eligible support for the following comparison under a specific tolerance.

(3) Through the comparison between two models, it was found that the *JF* factor of the improved model increases by 7,09 %, and the corresponding increases of heat transfer coefficient and pressure loss are 7,2 % and 0,07 %, respectively. This discovery might strongly back up the initial expectation of this work.

REFERENCES

[1] Ahmed S E A S, Ibrahiem Z. E., Mesalhy M. O., et al. Heat transfer characteristics of staggered wing-shaped tubes bundle at different angles of attack[J]. Heat and mass transfer, 50 (2014) 8, 1091-1102.

[2] Ahmed S E A S, Mesalhy M. O., Abdelatief A. M. Flow and heat transfer enhancement in tube heat exchangers[J]. Heat and Mass Transfer, 51 (2015) 11, 1607-1630.

[3] E. A S A S, M. O M, A. M A. Effect of Longitudinal-External-Fins on Fluid Flow Characteristics for Wing-Shaped Tubes Bundle in Crossflow[J]. Journal of Thermodynamics,254 (2015) 5, 1-16.

[4] Ahmed S E A S ,Mesalhy M. O., Abdelatief A. M. Heat transfer characteristics and entropy generation for wing-shaped-tubes with longitudinal external fins in cross-flow[J]. Journal of Mechanical Science and Technology, 30 (2016) 6, 2849-2863.

[5] Tahseen A. T., Ishak M., Rahman M. An overview on thermal and fluid flow characteristics in a plain plate finned and un-finned tube banks heat exchanger[J]. Renewable and Sustainable Energy Reviews, 43 (2015), 363-380.

Note: The responsible translator for English language is B. Z. Wang -NCST.